Aligned silane-treated MWCNT/liquid crystal polymer films

2008 Nanotechnology 19 175602

(http://iopscience.iop.org/0957-4484/19/17/175602)

Nanotechnology **19** (2008) 175602 (10pp) doi:10.1088/0957-4484/19/17/175602

Aligned silane-treated MWCNT/liquid crystal polymer films

Raoul Cervini[1], George P Simon[1], Milena Ginic-Markovic[2], Janis G Matisons[2], Chi Huynh[3] and Stephen Hawkins[3]

[1] Department of Materials Engineering, Monash University, Clayton VIC 3800, Australia
[2] School of Chemistry Physics and Earth Science, The Flinders University of South Australia, GPO Box 2100, SA 5001, Australia
[3] CSIRO Textile and Fibre Technology, PMB 10, Clayton, VIC 3168, Australia

Received 5 October 2007, in final form 25 February 2008
Published 25 March 2008
Online at stacks.iop.org/Nano/19/175602

Abstract

We report on a method to preferentially align multiwall carbon nanotubes (MWCNTs) in a liquid crystalline matrix to form stable composite thin films. The liquid crystalline monomeric chains can be crosslinked to form acrylate bridges, thereby retaining the nanotube alignment. Further post-treatment by ozone etching of the composite films leads to an increase in bulk conductivity, leading to higher emission currents when examined under conducting scanning probe microscopy. The described methodology may facilitate device manufacture where electron emission from nanosized tips is important in the creation of new display devices.

(Some figures in this article are in colour only in the electronic version)

1. Introduction

The development of new technologies for flat screens and architectural designs has been dramatic over the past decade. It has been predicted that silicon microchips will reach a physical barrier in 10–15 years, and extensive research is taking place to replace them by devices on the molecular scale [1]. Among such materials, carbon nanotubes (CNTs) have recently received much attention due to their striking mechanical and electrical properties. In particular, their quasi one-dimensional structures make them prime candidates for nanoelectronics applications [2]. Researchers worldwide are working on making transistors and other logic devices based on carbon nanotubes. IBM researchers, for example, recently reported CNT field effect transistors and intermolecular and intramolecular logic gates, realized using CNT bundles [3]. Their electrical properties in particular make them suitable for building a new generation of flat-screen displays called field emission displays (FEDs). FEDs work like conventional cathode ray tubes, except that each pixel is illuminated by its own electron source, which could well be made up of a very large number of well aligned carbon nanotubes. Many such applications require the growth of aligned and/or micropatterned carbon nanotubes with or without a chemically modified nanotube surface. The growth of aligned nanotubes via chemical vapour deposition (CVD) technology poses its own problems as its high temperature (about 650 °C) rules out many substrates, not least flexible polymeric ones [4–6] which would allow subsequent ease of device production; in addition, the lateral size on which it is possible to grow such 'forests' of nanotubes by CVD is quite limited. Attempts at aligning nanotubes in composite systems using polymeric matrices have also often proven unsatisfactory. Generally, a vertical alignment (perpendicular to the film surface) is desired to enable electron emission from the nanosized tip; this configuration is much more complex to achieve than the case where the CNTs would lie parallel to the film. Attempts to manipulate nanotube alignment have involved a variety of methods, including attempted alignment in the presence of strong magnetic [7] and electric fields [8], mechanical stretching [9], and shear forces and liquid flow [10]. All of these methods, however, rely on an external force to act on and orientate the nanotubes. Much more preferable would be processing techniques for electronic devices which are based on stable solution-processable routes, allowing low-cost fabrication, large-area coverage, and low processing temperatures on flexible substrates. Very recently there have been a few reports [11, 12] of using liquid crystals (LCs) as the alignment medium to control nanotube alignment; however, some of the processing methods are quite involved and require a pre-layer of aligned polyimide chains. In addition, the use of liquid crystals (as opposed to liquid crystalline polymer

systems) requires an aligning voltage to maintain mesogenic (and thus nanotube) orientation. In this work the MWCNTs are dispersed in a liquid crystalline monomer which is polymerized into a crosslinked matrix which retains the chain alignment. Homeotropic alignment of a liquid crystal occurs when the long axes of the molecules of the liquid crystal phase are, on average, essentially normal to the substrate upon which they form a thin film [13]. Very few materials spontaneously align in this way and usually some kind of aligning agent is required to produce this desired alignment. The nematic liquid crystalline material used in this work, and now the subject of a recent Merck patent, has the unique ability to self-align, and hence to impart a template directing effect on the MWCNTs [14]. A further key aspect of nanotube processing describes a method to facilitate superior dispersion of the nanotubes in the liquid crystal medium. In the context of device manufacture, inter-nanotube separation is a pivotal requirement within the matrix for high emission current and low turn-on voltage. The described method to chemically modify carbon nanotubes works well in this application, but also has the capacity to be a very useful platform for CNT treatment in other applications where solubility, dispersive ability and long shelf life are required. In addition we show that oxidative MWCNT treatments actually increase the electrical conductivity by cross-shell bridging via sp^3 bond formation [15]. This is a desirable attribute in electron field emission applications.

We report here on a convenient method to treat and align a solution-processed film of MWCNTs in a stable liquid crystalline matrix produced from liquid crystalline monomer, thereby retaining the nanotube alignment for use in devices. In brief, CVD-grown MWCNTs were thermally treated and then chemically functionalized with aminopropylsilane to aid solution and film processing and glass adhesion, then mixed with a UV-crosslinkable liquid crystalline acrylate monomer [14]. This solution was used to dip-coat glass slides to produce thin, composite films of aligned MWCNTs. The film was subsequently crosslinked by UV irradiation to form an orientationally stable composite. This process thus provides a method to prepare very large, thin film areas of aligned nanotubes on glass or flexible polymeric substrates by screen printing processing. The electrical properties and the high aspect ratio morphology of the nanotubes is maintained, and can be verified by a range of techniques such as electron microscopy, and other spectroscopic and electrical conductivity measurements. In this work MWCNTs (rather than single-wall CNTs) have been chosen for a number of reasons. Most importantly, their multi-layered nature means the outer surface can be readily modified, leaving the inner tubes untouched and electron emission largely unaffected.

2. Experimental details

The reactive mesogen mixture of monomers with acrylate side groups was obtained from Merck. It contains four main monomeric components: 4-(6-acryloyloxyhexyloxy)benzoic acid(4-(trans-4-propylcyclohexyl)phenyl ester), 4-(3-acryloyl-oxylpropyloxy)-benzoic acid-methyl-1,3-phenylene ester, 2-methyl-1,4-phenylene-bis[4-(6-acryloyloxyhexyloxy)benzo-ate], 4-(6-acryloyloxyhexyloxy)-benzoic acid (4-cyanophenyl ester). This mixture has 1% UV initiator (Igacure 907) to carry out the crosslinking of the acrylate groups. The films were crosslinked using a medium pressure Hg lamp. Film thickness was a key component in obtaining a well aligned film. With this unique material, homeotropic alignment is a function of film thickness. Vertical alignment in which the axis of the LC molecules is perpendicular to the substrate was identified by observation on a polarizing microscope and clearly differenti-ated between a poorly aligned and a well aligned sample. With films less than 5 μm thick the extinction under the polars did not change upon rotation of the sample; this is because the axis of the homeotropically aligned LC molecules is perpendicu-lar to the viewing direction. Such alignment was not observed in the isotropic phase where the film thickness is greater than 5 μm. An optimum film thickness of 2–5 μm was thus used to achieve self-alignment [14].

MWCNTs were produced by CSIRO TFT, Clayton, via a continuous catalyst injection CVD process using ferrocene (2%) in xylene at 750 °C with argon carrier gas. The CNTs grow as highly aligned forests on quartz substrates and have an average diameter of 100 nm and average length of up to 1000 μm. The x-ray photoelectron spectroscopy (XPS) spectrum of the as-received MWCNTs contained four carbon 1s peaks, at 284.6, 286.7, 290.4 and 285.3 eV, adding up to 99.7% atomic concentration; the quantification analysis also showed traces of iron (0.1%) and oxygen (0.2%). The detection limit of the machine is 0.1%. Thermal gravimetric analysis (TGA) at 2° min^{-1} in air up to 750 °C was carried out to determine the percentage weight loss. This revealed only 5% weight remained after the completion of the analysis. Critically, most weight (80%) was lost between 550 and 650 °C. Thus the 5 wt% is likely to be from Fe_2O_3, which equates to about 3.5% iron content. Qualitative visible evidence suggests a clean sample with no loose amorphous carbon visible.

The acids used for the reflux of the MWCNTs, H_2SO_4 (density, 1.84) and HNO_3 (density, 1.4), were obtained from Aldrich. The organic solvents, toluene (AR), cyclohexanone (AR), and absolute ethanol (AR), and the silicon coupling agent, aminopropyltriethoxysilane, were obtained from Aldrich. Thermal processing of the MWCNTs was carried out in 95% nitrogen in a tube furnace, calibrated with an external thermocouple. A Sonics ultrasonic wand, 750 W, was used for the dispersion processing of the nanotubes.

Samples were directly spin-coated onto gold substrates for XPS analysis, which was carried out on a Kratos AXIS Ultra machine (Kratos Analytical Ltd., UK) equipped with a monochromatized x-ray source (Al Kα, $h\nu$ = 1486.6 eV) and radiation at a source power of 150 W and a takeoff angle of 30° relative to the sample surface. The analysis areas were nominally 700 × 300 μm^2. Acquisition parameters for the wide scans were: pass energy 160 eV, mono aluminium anode, 150 W, 1 eV step, 200 ms dwell. The parameters for the high resolution scans were: pass energy 20 eV, mono aluminium anode, 150 W, 0.1 eV step, 200 ms dwell, providing

a sensitivity of 1.35 Mcps and a resolution of 0.577 eV for Ag 3d FAT20. Charge compensation was corrected with carbon 1s at 284.6 eV.

Near-infrared spectroscopy was carried out using a PerkinElmer Spectrum GX machine. Raman spectroscopy was carried out on a Almega XR dispersive visible Raman microscope (633 nm wavelength, He–Ne laser, 2 mW) and the beam was focused onto the specimen surface through a 50× objective lens, forming a laser spot of 2 μm in diameter. The spectral resolution of the experimental set-up is 2 cm^{-1}. The intensities of the characteristic MWCNT modes were monitored as a function of incident polarization. The scattered light from the sample is passed through an analyser that selects light that has the electric vector parallel to that of the incident light. Sample films were prepared on gold substrates. Conductive scanning probe microscopy (SPM) was carried out with a Joel JSTM 4200A.

2.1. Thermal oxidative treatment

The best condition to achieve functionalization by this method was a gentle oxidation in 95% nitrogen at 500 °C for 3 h, followed by ultrasound treatment for up to 1 h. The average weight loss was 6% after the 3 h period as extracted from TGA analysis at an isothermal temperature of 500 °C. The nanotubes were then suspended in absolute ethanol, 20% by weight, and ultrasonically pulsed for 1 h to fine-tune the length of the tubes. The nanotubes were collected by centrifuging at 20 000 rpm. Two layers were obtained: a sediment, 30% (longer nanotubes), and a suspension, 70% (shorter nanotubes). The suspension was evaporated to dryness and used for subsequent experiments.

2.2. Preparation of 3-aminopropyltriethoxysilane modified nanotubes

Further modification of the nanotubes was carried out to make them more compatible with the LC monomer mixture. In this case the nanotubes were refluxed in a mixture of concentrated acids, sulfuric/nitric in the ratio of 3:1, for 8 h in order to produce hydroxy and carboxylic defects in the carbon atom lattice. The reflux suspension was poured carefully into distilled water, and filtered on PTFE 0.45 μm Millipore filters. The resulting filter cake was dried *in vacuo* for 48 h at 80 °C; 80% by weight of nanotubes were recovered. Preparation of 3-aminopropyltriethoxysilane modified nanotubes involved forming zwitterions between the amine and the carboxylic groups of the nanotubes. Carboxylic modified nanotubes (120 mg) were suspended in absolute ethanol and pulse sonicated for up to 2 h to obtain a suspension of nanotubes. To the suspension, an excess of 3-aminopropyltriethoxysilane was added, and the pH was adjusted to 4.5 using dilute acetic acid. This mixture was allowed to stir at a constant temperature of 65 °C for 4 days. The mixture was then filtered on PTFE filters, and washed with absolute ethanol. The solid was then resuspended in absolute ethanol and centrifuged (Hettich universal) for 3 h at 7000 rpm. Two layers were again obtained, a sediment and a suspension. Both components were dried *in vacuo* and used for further experiments.

2.3. Preparation of thin composite films

Up to 5 wt% compositions were made using modified MWCNTs. The nanotubes were first suspended in a solution of absolute ethanol, and sonicated for 30 min. Separately the LC monomer mixture was suspended in absolute ethanol (40 wt%) and sonicated for 10 min. The two mixtures were combined and then sonicated for a further 30 min. The resulting mixture was then used to prepare the composite films on either borosilicate glass or F-doped SnO_2 glass, using a dip-coating process. UV irradiation at 365 nm was used to crosslink the films. Profilometry (Dektak) studies were used to experimentally determine the film thickness. In a similar process 5 wt% compositions were made using oxidized MWCNTs with PMMA (M_w, 50 000); tetrahydrofuran was used as the solvent.

3. Results and discussion

3.1. Electron microscopy of the composite nanotube films

The MWCNTs used were grown as templated forests with an average diameter of 100 nm, and lengths of up to 1 mm, (figure 1(a)). It is widely accepted that some form of post-processing of such nanotubes is required if they are to be incorporated into a polymer composite to prevent aggregation and ensure that the MWCNTs are homogeneously and individually dispersed throughout the matrix [16–18]. To this end, we report a new way to functionalize the nanotubes. A gentle thermal oxidation treatment was first used to disentangle the nanotubes, followed by acid etching and ultrasonication to cut the nanotubes into smaller rigid segments, optimally 5–7 μm. Such shorter, rigid, and distinct MWCNTs are desirable if a regular array of nanotubes is required. The acid washings and sonication processes commonly utilized to purify the nanotubes also create open end termini in the structure, which are stabilized by –COOH and –OH groups which bond to the nanotubes at the end termini or at sidewall defect sites [15, 16]. Following such treatment, the nanotubes were separated and collected by centrifuge; the mother liquor suspension obtained was dried *in vacuo* and inspected in both a scanning electron microscope (SEM) and a transmission electron microscope (TEM). The images show the MWCNTs at these different stages of processing.

3.2. Processing of MWCNTs

The use of MWCNTs over SWCNTs is preferred, as the electrical properties are found to actually be enhanced using chemical and thermal processing in multiwalled systems; furthermore, there is evidence suggesting the degradation rate of MWCNTs under field emission is much less than that of SWCNTs [19]. From our results we have found that thermal treatments (and especially acid etching) of these MWCNTs causes an increase in the DC electrical conductivity (pressed pellet four-probe measurement), presumably by decreasing the energy barrier for intershell carrier transport [20].

The acid-etched nanotubes were found to be able to be adequately dispersed in the liquid crystal monomer in a

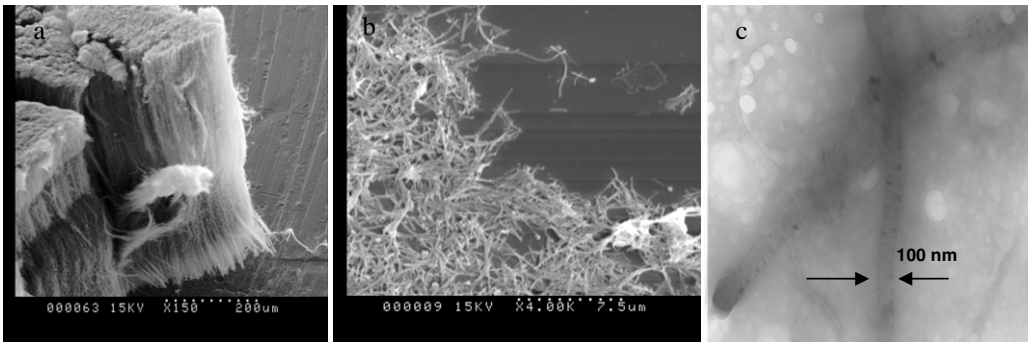

Figure 1. (a) Scanning electron microscope (SEM) image of as-synthesized forest arrays on the original substrate. The MWCNTs harvested are approximately 1 mm long and 100 nm in diameter. (b) Scanning electron microscope (SEM) image of MWCNTs after thermal treatment at 500 °C for 3 h under an atmosphere of 95% nitrogen/5% oxygen and chemically etched using H_2SO_4/HNO_3. (c) Transmission electron microscope (TEM) image of MWCNTs. The diameter of these nanotubes is 100 nm.

mixture of toluene–cyclohexanone (figure 3(a)). However, further derivatization of MWCNT–COOH increased the solution stability over time, decreased the aggregate size, and increased the wetting ability of the substrate during the dip-coating process. This further treatment of the acid-etched MWCNTs was achieved with 3-(aminopropyl)triethoxysilane (APTES). Two major products were obtained, a sediment and a suspension, as explained above. The suspension was used for the composites. The sediment contains a mixture of siloxane polymer and nanotubes. The suspension was material was analysed by Fourier transform infrared (FTIR) spectroscopy and XPS.

This above process gives rise to even better dispersion, and the composite can be processed in a much more benign solvent, ethanol. Ethanol was found to adequately disperse both the modified nanotubes and the LC monomer; toluene/cyclohexanol works just as well, but ethanol is a more benign solvent to use. Furthermore, ethanol proved to be a better solvent in terms of wetting the glass surface in preparation of the thin film composites. The mechanism of the observed solubility of MWCNTs in APTES is likely due to the formation of a charged amine carboxylate salt, $(MWCNT–CO_2)^{-+}(NH_3)(CH_2)_3Si(OH)_3$. The ammonium ion is not able to interact with the silanol; each moiety thus retains an associated zwitterion group [21]. The high concentration of polar groups infers that many must be at the surface, making it quite polar, which is assumed to be attracted to the polar glass surface. A similar mechanism of non-covalent donor–acceptor interaction has recently been proposed to explain the doping effect of carbon nanotubes in polyaniline composites [18], but this is the first time it has been reported using aminopropylsilane units with modified COOH–MWCNTs. This makes it a very useful platform for a range of CNT treatments and composites, given the wide range of silanes commercially available. This processing step is an important factor to consider when making large surface area films, and it allowed strongly adhering films of high quality to be able to be routinely processed using the steps outlined above. The functional groups on the modified nanotube surface were confirmed by high resolution x-ray photoelectron spectroscopy (XPS). Important peaks found in the XPS spectrum include: N 1s NH_3^+, 401.7 eV; C 1s, COO, 288.3 eV; C 1s C=O, 286.6 eV; O 1s Si–O, C–O, 532.5 eV; and Si 2p, Si–O, 102.780 eV.

Atomic concentrations obtained from multiplexed spectra were used for the calculation of the ratio of carbon/nitrogen. The atomic concentration % ratio of the charged amine group $(NH_3)^+$ to that of MWCNT–COO^- was 1.2, which means that most of the free carboxylic groups react with the amine terminated group. Other functional groups identified were carbonyl and hydroxyl; no free NH_2 groups were identified. The FTIR spectrum of MWCNT–APTES displayed bands at 3000 and 2800 cm^{-1}, corresponding to stretching of –CH. Carboxylic group stretching (–COO–) appeared at 1400 cm^{-1}. Stretching of amine salt ($-NH^-$) appeared at 3200 cm^{-1}, and the bending of the amine salt ($-NH3^+$) appeared at 1610 cm^{-1} and 1500 cm^{-1}. Absorption peaks at wavenumbers 1110 cm^{-1} and 950 cm^{-1} corresponded to –SiO– stretching.

The MWCNTs treated with APTES were used to make nanocomposites by combination with a UV-crosslinkable acrylate material. This commercial material is a liquid crystal monomer with reactive functionalities and it displays a readiness to spontaneously align homeotropically (perpendicularly) [14] to the glass surface onto which it is applied. This is very convenient as it appears not to require any prior surface treatment to cause such an LC alignment to a substrate surface. Up to 5 wt% of MWCNT–APTES could be dispersed within the liquid crystal monomer, and processing was still able to be easily carried out in absolute ethanol. Ultrasonic mixing for 30 min of MWCNT–APTES and monomer was required for complete mixing, and this solution showed no signs of instability after one year. With regards to applying films, individual glass segments were cleaned in acetone and a specified area masked with Scotch tape and dip-coated at a rate of 2 cm min^{-1} to give films of between 4 and 5 μm in thickness. A UV light of wavelength 365 nm for 2 min was used to crosslink the monomer, the final films being grey to black but remaining transparent at 5 wt% and strongly adhering to the glass surface.

The high magnification optical photograph in figure 2(a) illustrates a thin film on glass of the dispersion of MWCNT–COOH in the LC polymer While most of the MWNT material

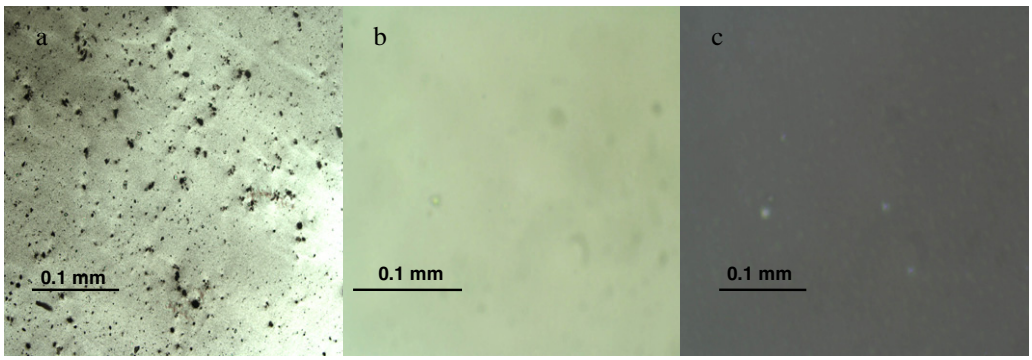

Figure 2. Optical microscopy of thin composite films. (a) A thin film of LC–MWCNT–COOH: the image shows a range of size of nanotube aggregates; there are some areas of good dispersion. (b) An LC–MWCNT–APTES film with excellent dispersion with minimal aggregates; the absence of visible CNT bundles in 3(b) shows that the bundle size is below optical wavelengths. (c) An LC–MWCNT–APTES film: qualitatively the film appears black between crossed polarizers, providing evidence that the LC director chains are aligned homeotropically to the substrate.

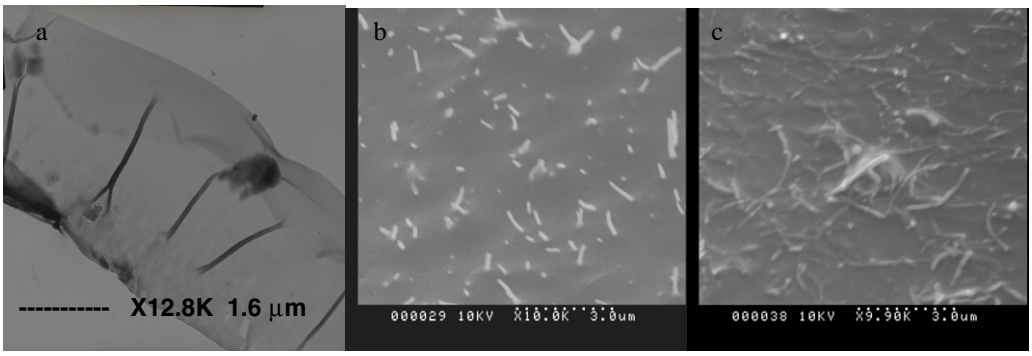

Figure 3. (a) A transmission electron micrograph (12.8k magnification) of a microtomed slice (50 nm) showing a series of aligned MWCNTs within the matrix. (b) An SEM image of the surface of a 5 μm LC–MWCNT–APTES composite film (2.5% MWCNT–APTES by weight). The nanotubes remain well separated and, importantly, protrude from the surface. The composite film area is 1.5 cm^2; thus from this SEM image the concentration of surface nanotubes is 1.5 $\times$ 107 cm^{-2}. (c) An SEM image of the surface of a 5 μm PMMA–MWCNT composite film (2.5% MWCNT by weight).

appears to be well dispersed, small aggregates of up to 10 μm are still observed in the mixture. Further improvement in the nanotube dispersion was achieved by extra processing of the MWCNT-COOH tubes with APTES, as described above. Figure 2(b) shows the excellent dispersion characteristics of this dispersion; the absence of visible MWCNT bundles in 2(b) shows that the bundle size is below the optical wavelength. Figures 2(b) and (c) also show the polarizing microscopy textures of the composite films and are qualitative evidence that the LC polymer aligns homeotropically to the substrate surface [14]. Representative scanning and transmission electron micrographs of aligned MWCNT–APTES in the LC matrix are shown in figures 3(a)–(c). The TEM image shows a small segment of composite film that was peeled from the underlining glass substrate and placed vertically in an epoxy setting resin; after curing, 50 nm slices were cut using a diamond knife. The slices were placed on copper grids for examination. The image shows a group of vertically aligned nanotubes. Figure 3(b) displays the surface topography of LC–MWCNT–APTES; a well separated aligned series of nanotubes can be seen to protrude from the polymer surface by approximately 2 μm as a consequence of a very thin polymer film, excellent dispersion and the templating effect of the LC director. Indeed such a surface is thought to be ideal for an electrical emitter. The distinction of dispersion and templating effect can be clearly observed from figure 4(c), which represents a composite film of MWCNTs in a non-liquid crystalline polymer, poly(methylmethacrylate), $M_w \sim$ 50 000. The film thickness is the same as that of the LC nanocomposite material (5 μm); thus any variation in alignment is solely due to the dispersion/templating effect of the LC and silane modified MWCNTs. Figure 3(c) shows a significant disruption to orientation and furthermore displays many bundled nanotubes.

3.3. Spectroscopy of LC–MWCNT–APTES films

It has previously been shown that resonant Raman spectroscopy can be used to determine the optical anisotropy of carbon nanotubes within composite films [22–24]. This is an excellent technique for assessing MWCNT alignment because the intensities of the MWCNT scattering modes are highly dependent on the degree of parallel interaction between the nanotube axis and the direction of the exciting laser light

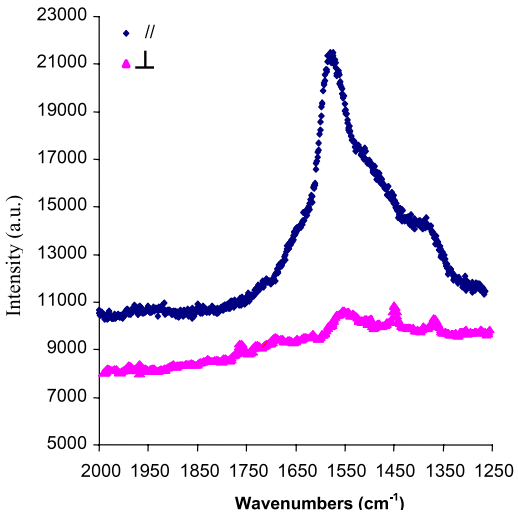

Figure 4. The MWCNTs of a thin film of LC–MWCNT–APTES (2.5 wt%) showing the G-band intensity with polarization, parallel and perpendicular, respectively, to the direction of the sample direction.

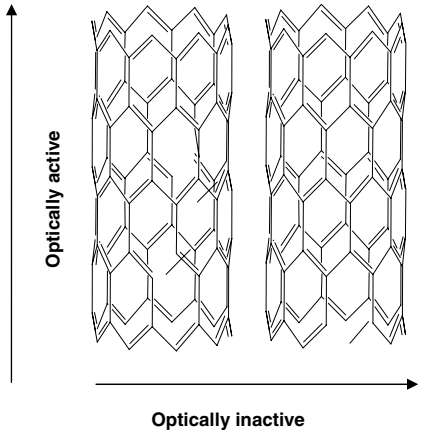

Scheme 1. A simple depiction of the optical anisotropy of carbon nanotubes. Due to structural anisotropy, the optical properties of the MWCNTs change depending on the direction of polarization.

(scheme 1) [25]. In this study we have used polarized Raman spectroscopy to look at the MWCNT alignment along the nematic director LC chains. In this case the Raman response with respect to polarizing angle of the laser light of a thin composite film of LC–MWCNT–APTES is shown in figure 4. The intensity of the G band (arising from the in-plane vibration of the C–C bonds) is a good indicator of MWCNT orientation with a composite film. The spectra at different angles were collected with the same experimental parameters except the change in the sample orientation. Figure 4 shows the Raman spectra taken with different polarizations at two different angles (0 and 90°). The G-band intensity, at 1575 cm^{-1}, is much greater when the light is polarized parallel to the LC template direction, thus indicating that the nanotubes are aligned along the LC director chains, as shown in scheme 2.

The resultant aligned composite films are optically homogeneous and display MWCNT-specific light absorption, which is attributable to the inter-band optical transitions in semiconducting MWCNTs [26]. Further evidence of the in-plane anisotropy of these films was gained by using polarized near-infrared absorption spectroscopy. Figure 5 displays the graphs for LC–MWCNT–APTES. It was found that the intensity of absorption in the near-infrared differs, depending on the direction of the light polarization, parallel (∥) or perpendicular (⊥) to the direction of the tube alignment. The absorption features disappear when the light is polarized perpendicular to the substrate direction. There is a synergy between better dispersion of silane-treated nanotubes and the directing effect of the LC polymer chains.

Thus the intensity of the inter-band semiconducting transitions of MWNTs with polarized excitation is another indicator of the nanotube orientation. The absorptions are due to optical transitions between van Hove singularities in the valence and conduction bands of various MWCNTs [27]. When the incident light is parallel to the orientation direction a number of inter-band nanotube absorption features are seen due to the structural anisotropy present in the film. The optical properties of the MWCNTs change depending on the direction of polarized light. Furthermore, the fact that such absorption features are observed indicates that individual silane-treated nanotubes are very well dispersed with the LC polymer. The absorption features decrease somewhat with the LC–MWCNT film, but some degree of alignment is still present due to the influence of the templating LC chains. Others have used such spectroscopic methods to probe the orientation of nanotubes produced by different methods. Kim *et al* [28] reported a technique to fabricate a highly aligned ensemble of isolated nanotubes in gelatin by mechanical stretching of the matrix and showed that it also exhibited highly polarized absorption. They found strong anisotropy when the electric field of the light is parallel or perpendicular to the tube axis. In particular they found there was preference for strong absorbance when the light is parallel to the carbon nanotube axes, and Zhao *et al* [29] recently confirmed such dispersions using *ab initio* calculations. The additional aspect of polarization allows a significant possibility that the optoelectronic functions of MWCNTs can be exploited in addition to enhancing the understanding of their electronic properties.

3.4. DC electrical conductivity measurements of composite MWCNT films

The anisotropic distribution of nanotubes in the LC polymer matrix was also confirmed through measuring the electrical conductivity in the directions perpendicular and parallel to the orientation of the polymer LC. Films of a non-aligning polymer (PMMA, M_w 50 000) and MWCNTs were also prepared for a comparison study. The first method used the four-probe linear probe technique using an in-house four-point spring loaded probe, a constant current source, and digital multimeter (Keithley 617, DMM). Such a measurement largely involves electron transport parallel to the film surface, and measures electrical transport within the upper layers of the material for a conductive material [30–32]. The electrical conductivities

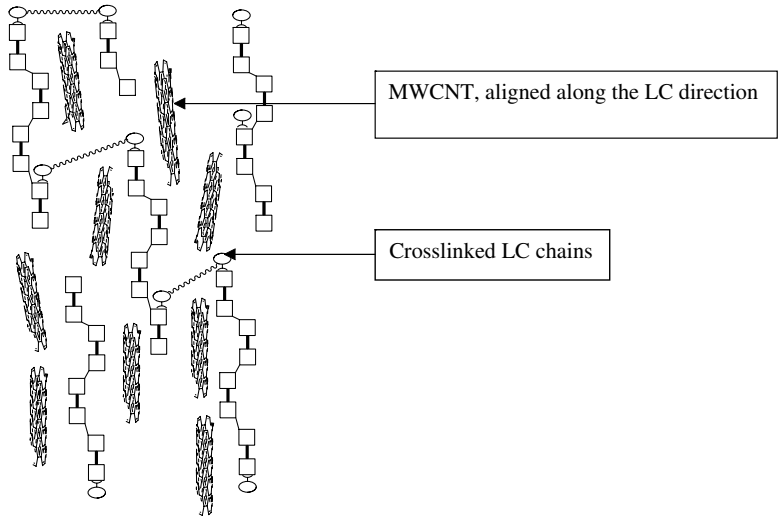

Scheme 2. This representation shows the preferred alignment of MWCNT–APTES when templated with crosslinked LC polymer chains.

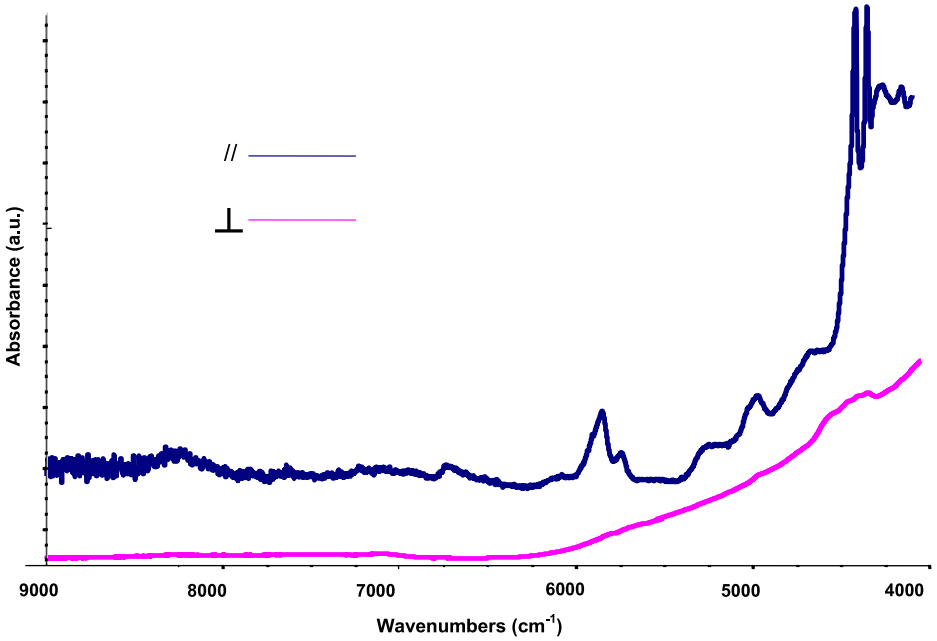

Figure 5. The polarized near-infrared absorption spectra of an aligned LC–MWCNT–APTES composite film (5 μm), showing the difference in absorption intensity with polarizing angle.

were calculated using the relation

$$\sigma = (\ln 2/\pi d)(I/V)$$

where d is the thickness of the film (measured by profilometry). Rectangular samples of dimensions 5×15 mm^2 were used, and the spacing of the spring loading probes was 1.5 mm.

The second method involved a two-probe square probe arrangement, in which measurement is made through the thickness direction. This configuration is a sandwich set-up and it requires the film to be cast on a conducting fluorine-doped SnO_2 film, which acts as an electrode. The top face of the composite film was used as the second electrode and was gold sputtered. The electrical conductivities were calculated using the relation

$$\sigma = d/A(I/V)$$

where A is the area of the electrode. For the two configurations the ohmic nature of the contacts was established from the linear nature of the current–voltage curves. At least five data points were obtained for each film sample to verify that Ohm's law was obeyed.

The two approaches to measure electrical conductivity are thus able to readily determine whether any electrical anisotropy is present in the LC–MWCNT–APTES films, and hence would indicate the structural templating effect of the liquid crystal polymer on nanotube alignment. Figure 6 displays two curves depicting the surface and volume conductivities for the LC

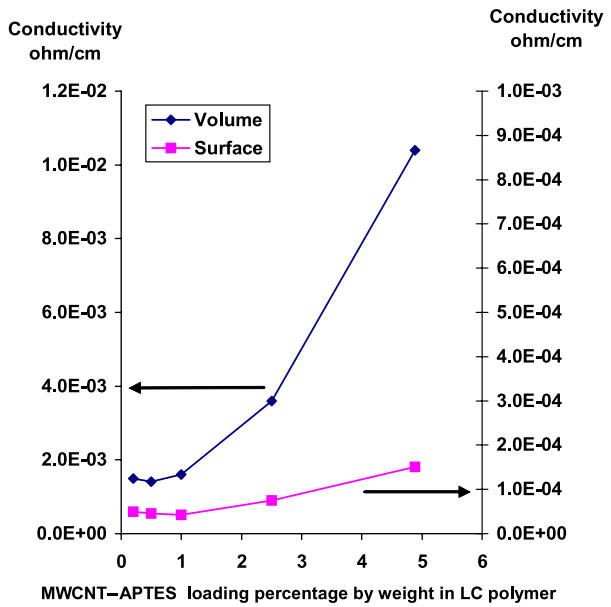

Figure 6. The DC electrical conductivity versus MWCNT–APTES loading in LC polymer for 5 μm films on F-doped SnO_2 glass.

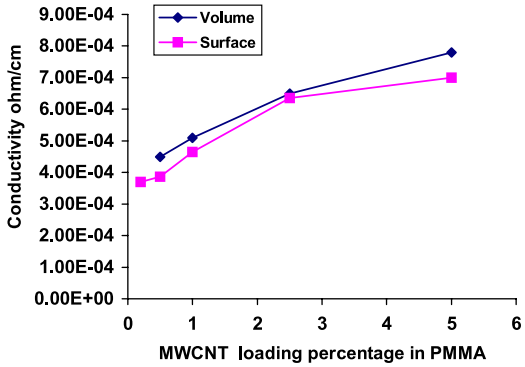

Figure 7. The DC electrical conductivity versus MWCNT loading in PMMA for a 5 μm film.

polymer system. The MWCNT–APTES loadings ranged from 0.2 to 5.0% by weight, with respect to the LC polymer. The volume (perpendicular) conductivity increases sharply around 1% loading, yet the surface conductivity remains constant and lower for each of the loadings. Measurements of the conductivity at different locations of the composite film gave consistent results. The difference in conductivity depending on direction indicates that electrical anisotropy is present, and hence a degree of structural alignment has been imparted to the nanotubes by the LC director chains. The increased conductivity suggests the nanotube alignment does indeed follow a perpendicular direction. In fact the nanotubes within the film form a head to tail conformation, thus ensuring interconnecting conduction pathways through the film. Conversely the lower surface conductivity implies that the nanotubes have preferential orientational order. The fact that the conductivity is still within the range 10^{-5}–10^{-4} Ω cm^{-1} suggests that the anisotropy is not absolute, and overlapping parallel nanotube connections occur in the matrix bulk. The opposite effect was observed with a film made with non-LC PMMA and MWCNT composite, as shown in figure 7, where there is no anisotropy of conductivity found. Since the surface and volume conductivities are the same, isotropic behaviour of the nanotubes residing within the non-templating medium, PMMA matrix, occurs. Furthermore, ohmic contact to the PMMA–MWCNT composite film varied depending on the electrode location, and this suggests highly aggregated areas and uneven distribution of nanotubes throughout the matrix, as can be seen by the morphological differences displayed in figures 3(b) and (c). It appears that the different properties of the two films are related to nanotube modification and subsequent degree of dispersion and the LC directing effect. The conductance behaviour shown in figures 6 and 7 provides further evidence that the alignment is genuinely related to the nanotube interaction with the liquid crystal host.

The ability to align nanotubes in a ensemble of aligning liquid crystal chains and then be able to lock in the orientation by crosslinking the matrix, as we report here, may seem surprising, even though we have shown a range of direct and spectroscopic evidence to support it. Recently Bliznyuk *et al* [11] have proposed a semi-quantitative model for nanotube alignment within an LC nematic director. They describe the observed anisotropy of physical properties in terms of anchoring of the polymer chains to the nanotube surfaces and adjustment of the nanotube orientation to the nematic direction. In the context of this study the carbon nanotubes are aligned by the small LC host phase and it would seem to be a fair presumption that there is a synergism between the two components with the host phase aligning the nanotubes and reciprocally with the nanotubes stiffening the LC phase. One would expect the host phase to impart some repulsion force (such as van der Waals) on the modified MWCNT–APTES. Both the LC chains and the nanotubes have polar moieties. In addition, hydrogen bonding between the free silanols on the modified nanotubes and the cyano groups on the LC would play a role in contributing towards the macroscopic alignment.

3.5. Post-treatment of composite MWCNT films using UV/ozone etching

A reactive oxidative gas, O_3, and UV energy were used to post-treat films of LC–MWCNT–APTES at elevated temperatures for 1 h at a rate of 2.5 L min^{-1}. UV-generated ozone has proven to be useful in the oxidation of carbon and silicon materials on a number of substrates. In this context the aim was to etch and heat the organic LC polymer to reveal more MWCNTs and hence provide a conductivity-rich surface for efficient electron emission. The volume conductivity was measured for the LC–MWCNT–APTES (2.5 wt%) films after ozone etching treatments. From figure 8 it can be seen that the conductivity of the composite film increases with increasing temperature of the ozone etching. The 250 °C sample has a conductivity of 25 Ω cm^{-1}, and the modified nanotubes measured as a pressed pellet have a conductivity of 175 Ω cm^{-1}. The morphology of the ozone-treated samples is shown in figure 9. It can be seen that the combination of ozone and heat degrades the LC polymer compared to the

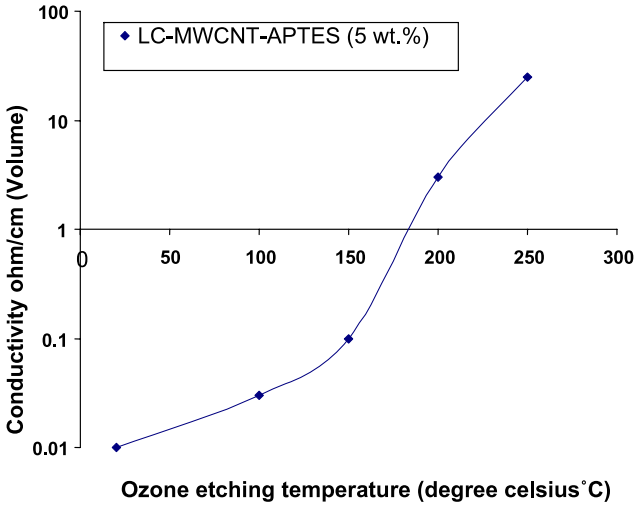

Figure 8. The graph displays a significant conductivity increase with ozone etching temperature.

untreated film in figure 3(b), and would probably have an effect on the aminopropylsilane side chains of the MWCNTs. It can be argued that etching of organic polymer film exposes more carbon nanotubes at the surface; in addition, the nanotubes that are exposed undergo functionalization to form oxygen-containing groups [33, 34]. This process, by itself, has been found to increase the conductivity of MWCNTs. The main reason why a large conductivity increase is seen is due to shedding polymer insulator from the nanotubes surface, thus creating better electrical connection to the probe electrodes. Although the conductivity is increased in these films it appears from the SEM images that the nanotubes are overlapping their neighbours, causing a high density of nanotubes, a feature which is usually unwanted in efficient electron emitters.

In the hope of retaining the nanotube surface structure such as that in figure 3(b), ozone etching was carried out on a composite film at room temperature. The film morphology on examination under the SEM is virtually the same as that in figure 3(b). The volume conductivity was measured and increased slightly compared to an unetched sample; remeasurement of the polarized Raman spectrum gave the same result as that from the unetched sample. The rise in conductivity means that the nanotubes have been 'cleaned' of wrapped polymer from their surface. Preliminary conductivity measurements on individual nanotubes within the LC matrix have been carried out using scanning probe spectroscopy. A non-etched and an etched film (not heat treated) have been compared. By scanning using a platinum tip, over a sample area of 2×2 μm, individual nanotubes were located at the composite film surface and a bias was swept across its region to deduce its I/V characteristics. The etched sample reproducibly returned higher emission currents and within the area scanned more nanotubes were detected. This reflects the efficiency of UV-ozone etching at room temperature to remove fragments of polymer from the tips, thus enabling the probe tip to make more contact area to the nanotube tip. Bulk electron emission studies are also currently in progress.

4. Conclusion

In conclusion, modified MWCNTs have been aligned by a template-assisted method using a homeotropically aligned liquid crystalline monomer that is subsequently polymerized to a rigid polymeric material, and leads to retention of the orientation of both the mesogen and (more importantly) the nanotube. The alignment is confirmed by electron microscopy, spectroscopy and by the observed anisotropy of electrical conductivity. Importantly (and usefully) the anisotropy increases with increasing concentrations of MWCNTs, and alignment is unique to the liquid crystal acrylate system, in comparison to the MWCNTs being random in orientation when the matrix of the composite is composed of isotropic, non-liquid crystalline, PMMA. The nanotubes that protrude from the LC matrix can be cleaned of excess polymer by ozone etching, making them more conductive and more suitable for an electron emitter device.

Acknowledgment

This work was supported by the Australian Research Council.

References

[1] Okazaki T and Shinohara H 2005 *Appl. Phys. Carbon Nanotub.* (Heidelberg: Springer) pp 133–50

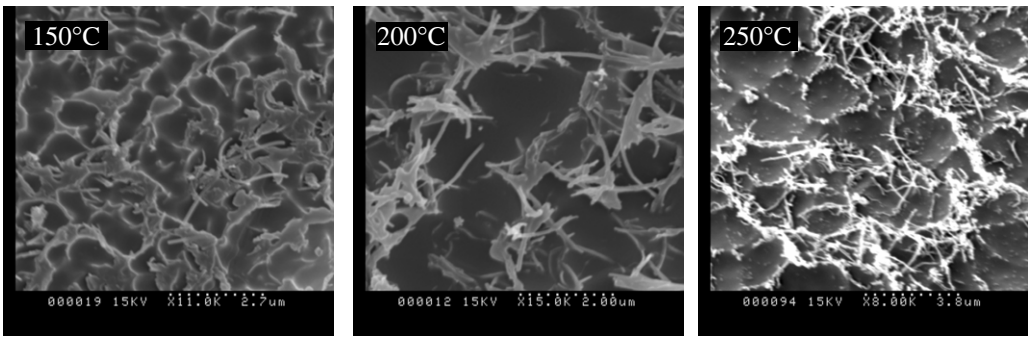

Figure 9. UV-ozone etching for 1 h at a rate of 2.5 L min^{-1} at elevated temperatures for LC–MWCNT–APTES films. The polymer matrix undergoes significant degradation, leaving behind a mass of carbon nanotubes.

[2] Guldi D M, Rahman G M A, Sgobba V and Ehli C 2006 *Chem. Soc. Rev.* **35** 471–87
[3] http://www.research.ibm.com/nanoscience/fet.html
[4] Gao M, Zuo J M, Zhang R and Nagahara L A 2006 *J. Mater. Sci.* **41** (14) 4382
[5] Ohnaka H, Kojima Y, Kishimoto S, Ohno Y and Mizutani T 2006 *Japan. J. Appl. Phys.* 1 **45** 5485–9
[6] Ding L, Zhou W, Chu H, Jin Z, Zhang Y and Li Y 2006 *Chem. Mater.* **18** (17)
[7] Choi E S, Brooks J S, Eaton D L, Al-Haik M S, Hussaini M Y, Garmestani H, Li D and Dahmen K 2003 *J. Appl. Phys.* **94** 6034–9
[8] Park C, Wilkinson J, Banda S, Ounaies Z, Wise K E, Sauti G, Lillehei P T and Harrison J S 2006 *J. Polym. Sci.* B **44** 1751–62
[9] Ichida M, Mizuno S, Kataura H, Achiba Y and Nakamura A 2004 *Appl. Phys.* A **78** 1117–20
[10] Camponeschi E, Florkowski B, Vance R, Garrett G, Garmestani H and Tannenbaum R 2006 *Langmuir* **22** 1858–62
[11] Bliznyuk V N, Singamaneni S, Sanford R L, Chiappetta D, Crooker B and Shibaev P V 2006 *Polymer* **47** 3915–21
[12] Dierking I, Scalia G, Morales P and LeClere D 2004 *Adv. Mater.* **16** 865–9
[13] Cognard J 1981 *Mol. Cryst. Liq. Cryst.* **78** (Suppl. 1) 1–77
[14] Merck Patent GmbH 2004 *US Patent Specification* 6816218
[15] Simmons J M, Nichols B M, Baker S E, Marcus M S, Castellini O M, Lee C-S, Hamers R J and Eriksson M A 2006 *J. Phys. Chem.* B **110** 7113–8
[16] Ni W, Wang B, Wang H and Zhang Y 2006 *J. Macromol. Sci.* B **45** 659–64
[17] Hwang S-H, Moorefield C N, Dai L and Newkome G R 2006 *Chem. Mater.* **18** 4019–24
[18] Liu J *et al* 1998 Fullerene pipes *Science* **280** 1253–6
[19] Jeong H J, Choi H K, Kim G Y, Song Y I, Tong Y, Lim S C and Lee Y H 2006 *Carbon* **44** 2809
[20] Sinnott S B 2002 Chemical functionalisation of carbon nanotubes *J. Nanosci. Nanotechnol.* **2** 113–23
[21] Litt M and Matsuda T 1975 *J. Appl. Polym. Sci.* **19** 1221–5
[22] Zengin H, Zhou W, Jin J, Czerw R, Smith D W Jr, Echegoyen L, Carroll D L, Foulger S H and Ballato J 2002 *Adv. Mater.* **14** 1480–3
[23] Kumar S and Bisoyi H K 2007 *Angew. Chem, Int. Edn.* **46** 1501–3
[24] Lagerwall J, Scalia G, Haluska M, Dettlaff-Weglikowska U, Roth S and Giesselmann F 2007 *Adv. Mater.* **19** 359–64
[25] Duesberg G, Loa I, Burghard M, Syassen K and Roth S 2000 *Phys. Rev. Lett.* **85** 5436
[26] Chen J, Rao A M, Lyuksyutov S, Itkis M E, Hu A H, Cohn R W, Eklund P C, Colbert D T, Smalley R E and Haddon R C 2001 *J. Phys. Chem.* B **105** 2525–8
[27] Landi B J, Ruf H J, Evans C M, Cress C D and Raffaelle R P 2005 *J. Phys. Chem.* B **109** 9952–65
[28] Kim Y, Minami N and Kazaoui S 2005 *Appl. Phys. Lett.* **86** 234
[29] Zhao G L, Bagayoko D and Yang L 2006 *J. Appl. Phys.* **99** 543
[30] Kiani M S and Mitchell G R 1993 *J. Phys. D: Appl. Phys.* **26** 1718–21
[31] Brown M A C S *et al* 1966 *Br. J. Appl. Phys.* **17** 1143–8
[32] *Am. Soc. Test. Mater* 1973 (Philadelphia: ASTM Standard) p F723 part 43
[33] Byl O, Liu J and Yates J T Jr 2005 *Langmuir* **21** 4200–4
[34] Mawhinney D B, Naumenko V, Kuznetsova A, Yates J T Jr, Liu J and Smalley R E 2000 *J. Am. Chem. Soc.* **122** 2383–4